Synthesis, Resolution, and Absolute Configuration of a Phosphine-Based Hemicryptophane Cage with an Endo Phosphorus Lone Pair and Formation of the Corresponding Gold Complex

Marc Hennebelle, Yoann Cirillo, Anne-Doriane Manick, Didier Nuel, Alexandre Martinez, Bastien Chatelet

Synthesis, Resolution, and Absolute Configuration of a Phosphine-Based Hemicryptophane Cage with an Endo Phosphorus Lone Pair and Formation of the Corresponding Gold Complex

Marc Hennebelle, Yoann Cirillo, Anne-Doriane Manick, Didier Nuel,* Alexandre Martinez,* and Bastien Chatelet*

ABSTRACT: The synthesis, characterization, and chiroptical properties of a new class of hemicryptophanes combining a phosphine moiety and a cyclotriveratrylene unit are reported. The synthesis was short and efficient. The racemic mixture of the cage was resolved by chiral high-performance liquid chromatography (HPLC), giving access to enantiopure molecular cages, whose absolute configurations could be assigned by electronic circular dichroism (ECD) spectroscopy. These new phosphines were then reacted with gold in order to make the corresponding enantiopure gold complexes. The X-ray structure reveals an endohedral functionalization of the cage with the gold metal entrapped in the heart of the cavity, leading to a V_{bur} of 58%. Moreover, the chirality of the cyclotriveratrylene unit was found to control the chiral arrangement of the aryl group linked to the phosphorus atom, located at the opposite side of the cavity.

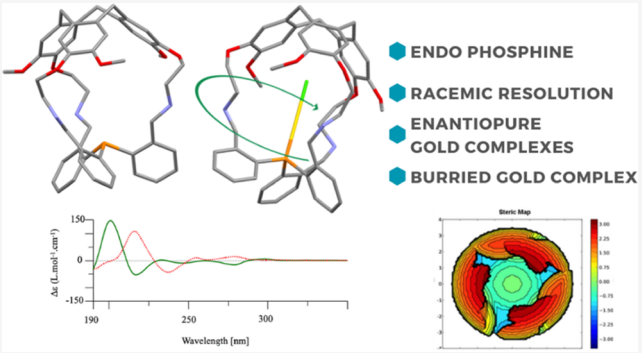

INTRODUCTION

Molecular cages have aroused great interest in the last two decades due to their various applications in catalysis, recognition, separation, and reactive species stabilization.[1] Inspired by nature, chemists designed nanoreactors possessing a molecular cavity, which can bind a substrate and accommodate a reactive center in order to mimic the efficient systems found in biological systems, such as enzymes.[2] These molecular flasks have been shown to impact the reaction outcome. However, devising cage compounds with endo functionalization remains challenging. Among the different cages, one can distinguish between the self-assembled and covalent cages. The former is made from small subunits that interact together to make sophisticated structures in just a few synthetic steps. Fujita was the pioneer, who reported remarkable examples of self-assembled cages.[3,4] Other groups such as those of Raymond,[5,6] Rebek,[7] Ballester,[8] Reek,[9] Stang,[10] Hardie,[11] and Nitschke[12] also reported significant examples of self-assembled structures with a functionalized cavity. Concerning the covalent host molecules,[13−18] few of them feature real endo functionalization. Among the ligands that have been incorporated into a cavity-shaped subunit, phosphines have aroused interest because the cavity can allow controlling the second coordination sphere of the related metal complex. Many examples with a phosphine unit confined in a cavity show a rather partial entrapment. Cyclodextrins or calixarenes bearing phosphine ligands have either the phosphorus moiety partially encapsulated or phosphine arms outside the cavity.[14,19] Jabin et al. reported the endo functionalization of calixarene with a phosphine ligand and the related copper complexes.[20] Nevertheless, all of these complexes display a funnel-shaped cavity, and a confined phosphine into a chiral bowl-shaped cavity has, to the best of our knowledge, not been reported yet. In this context, our group reported many examples of hemicryptophanes combining a cyclotriveratrylene unit and a C_3 symmetrical unit. We described several examples of cages bearing a tris(2-aminoethyl)-amine (tren),[21] trialkanolamine,[22] and tris(2-pyridylmethyl)amine (TPA) unit.[23] All of these moieties turned out to be successful to obtain functionalized cages. They can complex highly active metals in catalysis, such as iron complexes for the oxidation of alkanes,[15] or they have been applied successfully in the molecular recognition of compounds of biological interest, such as neurotransmitters.[24] We also previously reported Verkade's superbases confined into hemicryptophanes.[25] These molecules turned out to be active organocatalysts,

Scheme 1. Synthesis of Functionalized Aryl Phosphine 4

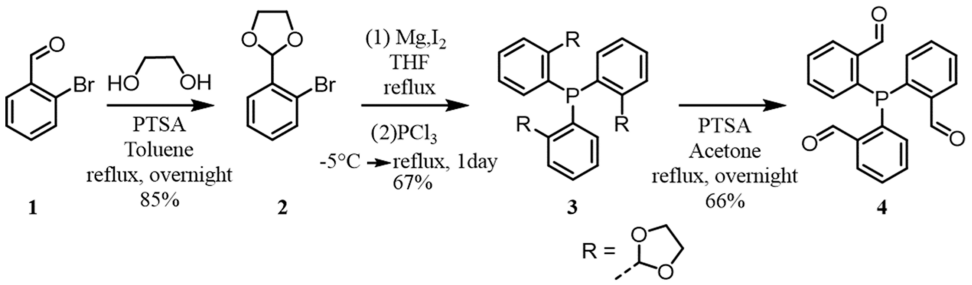

Scheme 2. Synthesis of the Racemic Mixture of Hemicryptophane 10

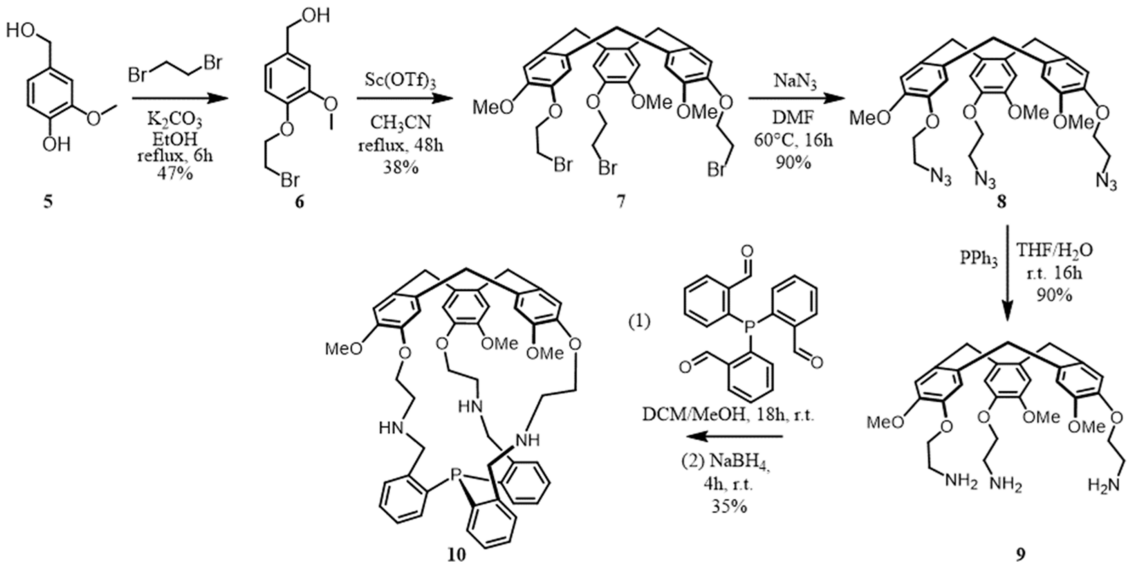

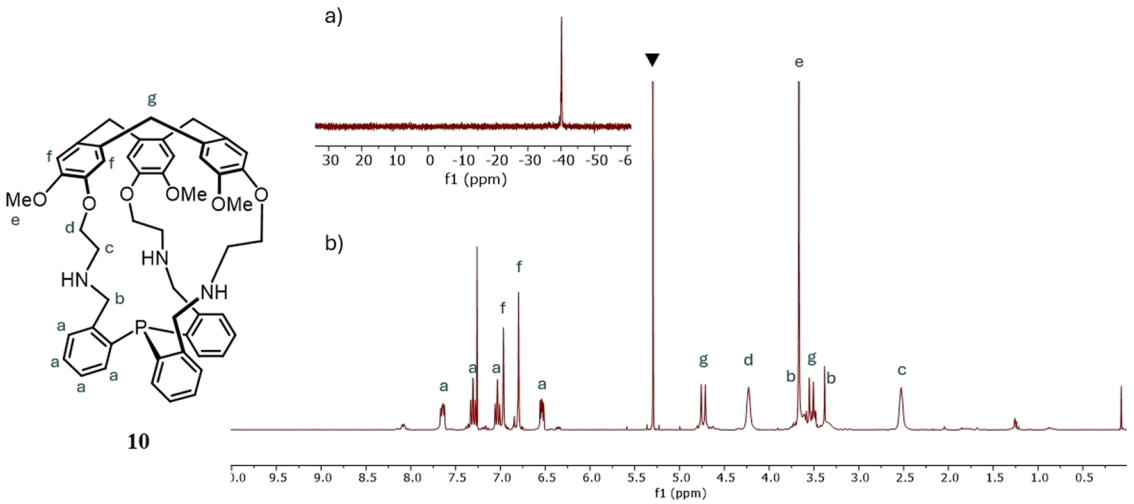

Figure 1. (a) ^{31}P and (b) ^{1}H NMR spectra of phosphine phosphine **10** ($CDCl_3$, 298 K, 162 and 400 MHz).

which proved to be more effective or more stable in comparison to the same molecules lacking a cavity.[26]

Knowing that examples of real endo phosphines are rare, we decided to synthesize a tertiary phosphine encapsulated into a hemicryptophane structure. The synthesis was achieved between a cyclotriveratrylene (CTV) unit, bearing three amine functions and an aryl phosphine with three ortho-substituted aldehyde functions. The racemic phosphine was resolved by chiral high-performance liquid chromatography (HPLC), leading to enantiopure substrates. Electronic circular dichroism (ECD) was used to determine the absolute configuration of each enantiomer cage. Then, we synthesized the confined gold complex by reacting the enantiopure phosphines with chloro(dimethylsulfide)gold(I), leading to the corresponding hemicryptophane gold complex.

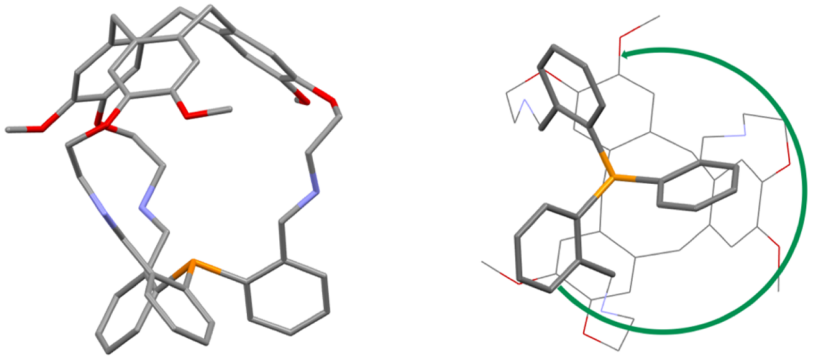

Figure 2. Diagram of the X-ray molecular structure of cage **10**. Green arrow: orientation of the three aromatic rings of the phosphine moiety.

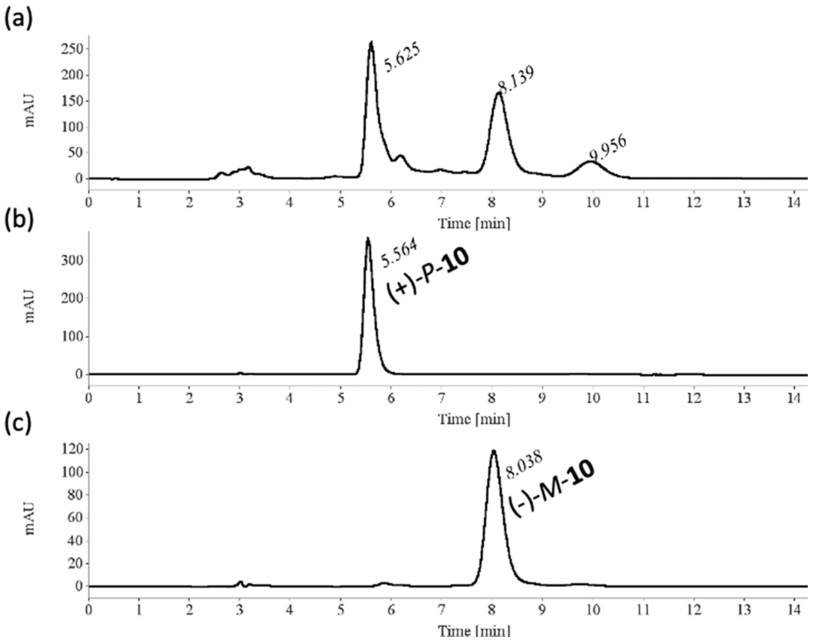

Figure 3. HPLC chromatogram of (a) the two enantiomers of **10**; (b) the first eluted enantiomer of **10**; and (c) the second eluted enantiomer of **10** (Chiralpak IG; eluent: heptane/ethanol/dichloromethane (30:30:40)).

RESULTS AND DISCUSSION

To synthesize the target hemicryptophanes, two different routes can be followed to obtain the cage compounds: (i) the first pathway involves a (1 + 1) coupling reaction between the CTV unit and another C_3 symmetrical part to afford the expected cage or (ii) alternatively, the CTV unit can be built during the last step of the synthesis. In this study, we focused on the former route: the coupling of the CTV moiety bearing three amine functions with a phosphine containing three aldehyde functions to form three imine bonds. Subsequently, the imine bonds formed were reduced to the amine functions. The first building block was synthesized according to the procedure described by Jabin et al.[20] The aldehyde function of 2-bromobenzaldehyde **1** is first protected with ethylene glycol, leading to acetal **2** in 85% yield. This compound was then reacted with magnesium to give the corresponding Grignard reagent, which can react with phosphorus trichloride to give the corresponding aryl phosphine **3** with a yield of 67%. Deprotection of the acetal function with *p*-toluenesulfonic acid then leads to the phosphine with free aldehyde functions (compound **4**) with a good yield (66%) (Scheme 1).[27] The other part of the cage consists of a CTV unit bearing three amine functions.

The synthesis of this building block starts from vanillic alcohol **5**, which was then reacted with dibromoethane to give compound **6**. Addition of scandium triflate to **6** in acetonitrile leads to CTV **7** with three arms with a bromine atom (18% yields over the two steps).[28] The nucleophilic substitution with sodium azide leads to compound **8** with three azide groups, which were reduced using PPh_3 to give the CTV with three amine functions **9**.[29]

The subsequent reaction of CTV **9** with functionalized phosphine **4** leads, after reduction of the imine bonds with sodium borohydride, to hemicryptophane **10** in 35% yield (Scheme 2). This synthetic scheme allows the preparation of cage **10** at a 200 mg scale. The ^{1}H NMR spectrum of **10** indicates that this cage is, on average, of C_3 symmetry in solution (Figure 1). The usual signals of the CTV unit were found, i.e., two singlets for the aromatic protons at 6.90 and 6.97 ppm, one singlet for the OCH_3 groups at 3.67 ppm as well as the characteristic AB system for the $ArCH_2$ bridges at 3.53 and 4.73 ppm with a typical coupling constant of 15 Hz. The aromatic protons of the phenyl groups display well-defined signals. The CH_2 signals on the linkers at 2.53 and 4.23 ppm display broad signals, possibly due to the flexibility of the linkers at room temperature. The ^{31}P NMR spectrum exhibits a single signal at

−41 ppm (Figure 1a), strongly shifted compared to triphenylphosphine (δ = −6 ppm). Single crystals of cage **10** suitable for X-ray diffraction were obtained by slow evaporation from a mixture of dichloromethane and methanol. The molecule shows a real endo functionalization with the phosphorus atom pointing inward toward the cavity (Figure 2). The structure reveals C_3 symmetry of the host as well as a helical arrangement of the three aromatic rings around the phosphorus atom. The CTV unit indeed strongly controls the chirality of the south unit: a CTV with a *P* (respectively *M*) configuration induces a Δ (respectively Λ) chirality of the propeller-like arrangement of the triarylphosphine moiety. This is in agreement with the ability of the CTV unit to control the helical arrangement of the linkers or of other south units like triamide unit[30] or tris(2-pyridylmethyl)amine (TPA) moieties.[23]

The hemicryptophane racemate was then optically resolved on a Chiralpak IG column (250 × 4.6 mm), with an enantioselectivity of 1.94 and a resolution of 4.61, using heptane/ethanol/dichloromethane (30:30:40) as the mobile phase (Figure 3). After multiple injections on a preparative Chiralpak IG column, 17 mg of the (+)-enantiomer and 18 mg of the (−)-enantiomer were obtained with ee values of more than 99.5 and 98%, respectively.

The absolute configuration of the enantiopure cages was determined by ECD spectroscopy recorded in acetonitrile at 298 K by comparison with already assigned hemicryptophanes.[31] As shown in Figure 4, the spectrum of the first eluted enantiomer

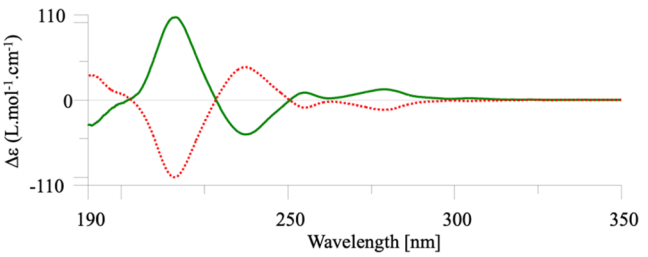

Figure 4. Experimental ECD spectra in acetonitrile at 298 K of (+)-*P*-**10** and (−)-*M*-**10**: first eluted enantiomer (+)-*M*-**10**: green solid line; second eluted enantiomer (−)-*P*-**10**: red dotted line.

exhibits a characteristic positive−negative bisignate curve from 230 to 250 nm (^1La transition) corresponding to the *M*-configuration. As expected, the second eluted enantiomer shows a mirrored ECD signal, allowing the assignment of the *P* configuration.

We then focused our attention on the ability of this confined phosphine to form the corresponding gold complex. The reaction of the phosphine with chloro(dimethylsulfide)gold(I) leads to the gold complexes with quantitative yields (Scheme 3).

The ^{1}H NMR spectrum of gold complex **10**@AuCl shows interesting features (Figure 5). The two singlets corresponding to the protons of the phenyl rings of the CTV unit in the aromatic region are slightly downfielded as well as the aromatic protons of the phenyl groups of the phosphine moiety. The previously broad signals of the diastereotopic aliphatic protons of the linkers are now well-defined after the formation of the gold complex and are split into two sets of signals. For instance, the broad signal at 4.23 ppm (−O-C$\underline{H}_2$-) gives two doublets of triplets at 3.82 and 4.31 ppm. This suggests a more rigid structure: the flexibility of the linkers and their free rotations are probably restricted by the steric hindrance induced by the gold ion within the cavity. The signal of the phosphorus atom coordinated to gold is downfield of 40 ppm in the ^{31}P NMR spectrum in comparison to the free phosphine (Figure 5). Crystals suitable for X-ray diffraction were obtained from slow evaporation of a solution of the gold complex in a mixture of dichloromethane and methanol. The structure reveals the encapsulation of the gold complex in the heart of the cavity (Figure 6). The complex exhibits C_3 symmetry in the solid state, in agreement with the ^{1}H NMR spectrum. As observed in the structure of the confined phosphine, the CTV with the *P* configuration (respectively *M*) imposes a Δ (respectively Λ) arrangement of the triarylphosphine unit. SambVca (2.0) software was used to determine the percentage buried volume; the **10**@AuCl complex displays a 58%V_{bur}. This constitutes one of the highest V_{bur} values ever reported for chloride gold complexes. The steric map depicts the contour of the catalytic pocket which can accommodate the substrate. The color scheme is employed to highlight regions within the catalytic pocket where the substrate can be accommodated either above or below the metal center[32a] (Figure 6). The value is indeed between the triphenylphosphine gold complex which possesses two phenyl groups in ortho position (V_{bur} = 53,6%) and the one with three phenyl groups (V_{bur} = 64,5%). This value is much higher than the one for the simple triphenylphosphine gold complex (V_{bur} = 30,8%).[32b] Finally, the enantiopure (+)-*P*-**10**@AuCl complex, prepared from optically resolved (+)-*P*-**10** phosphine, was analyzed by ECD spectroscopy (Figure 7). It can be observed that the complexation affects the ECD pattern. The structure of the complex is probably more rigid than that of the phosphine, as suggested by the NMR spectra (vide supra). Thus, the chiral arrangement of the aromatic rings of the phosphine might be retained in solution for the complex and not for the phosphine. Hence, this chiral south unit could also contribute to the overall ECD spectrum in solution, leading to some changes.

Scheme 3. Synthesis of the Gold Complex 10@AuCl

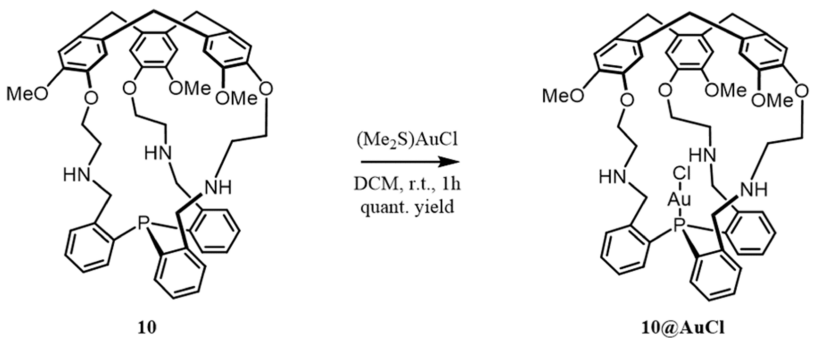

10 **10@AuCl**

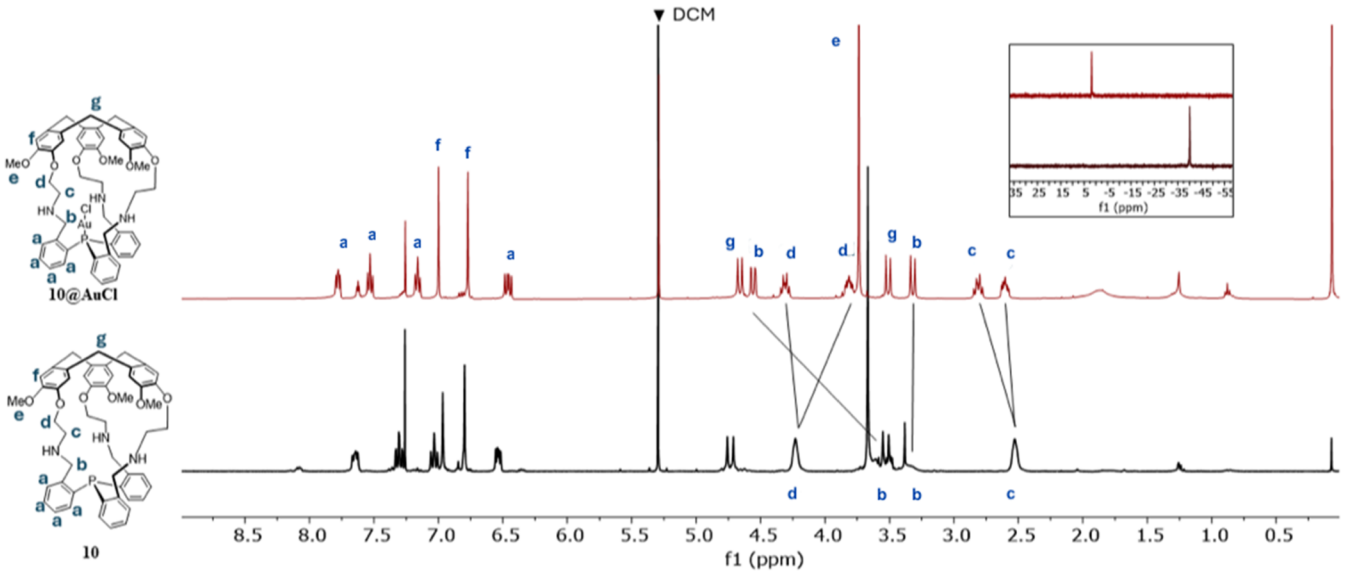

Figure 5. ^{1}H NMR spectra of phosphine **10** and gold complex **10**@AuCl ($CDCl_3$, 298 K, 400 MHz). Framed in black (top right): ^{31}P NMR spectra ($CDCl_3$, 298 K, 162 MHz), up: gold complex **10**@AuCl, down: phosphine **10**.

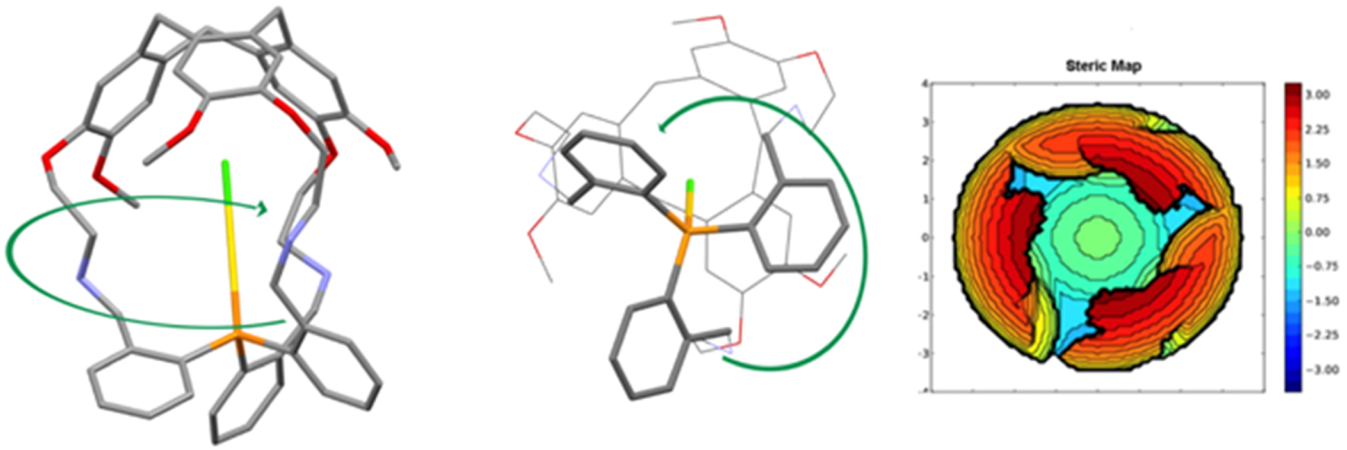

Figure 6. Diagrams of the X-ray structure of **10**@AuCl (left and middle). Buried volume $\%V_{bur}$ calculated for **10**@AuCl (right).

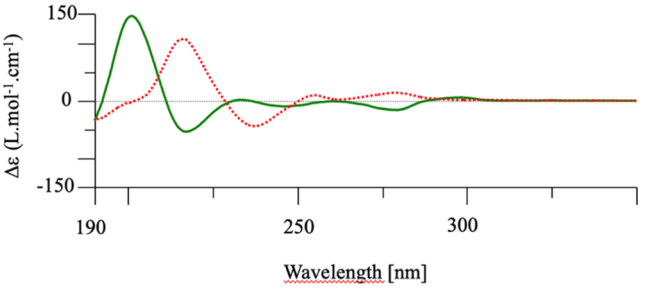

Figure 7. Experimental ECD spectra of (+)-*P*-**10** (red dotted line) and (+)-*P*-**10**@AuCl (green solid line) in acetonitrile at 298 K.

CONCLUSIONS

This study details the synthesis of a novel hemicryptophane compound, characterized by the incorporation of an endo phosphine unit. By employing chiral HPLC, racemic mixtures were effectively resolved, yielding enantiopure confined phosphine, whose absolute configurations were determined through ECD. Building upon this foundation, we delved into the synthesis of confined gold complexes, and NMR analysis unveiled a marked increase in structural rigidity upon gold complexation. Through the lens of X-ray crystallography, we gained valuable insights into the structural intricacies of both the cage phosphine and the resulting confined gold complex. Notably, our observations revealed an inward orientation of the lone pair of the phosphorus atom within the cavity, providing a structural basis for further exploration. Moreover, the chiral CTV unit demonstrated its ability to influence the chirality of the triarylphosphine moiety, establishing a compelling dual chiral coordination sphere.

EXPERIMENTAL SECTION

General Methods. Anhydrous solvents were obtained by filtration through drying columns (THF, Et_2O, and CH_2Cl_2). All reagents and solvents were of commercial quality and were used without further purification. Analytical thin-layer chromatography (TLC) was performed on plates precoated with silica gel layers (Merck 60 F254). Visualization of the developed chromatogram was followed by UV absorbance. Flash column chromatography was performed using 40−63 mesh silica. Nuclear magnetic resonance spectra were recorded on a Bruker AV 400 (at 400, 100, and 162 MHz, respectively, for ^{1}H, ^{13}C, and ^{31}P NMR spectra). Chemical shifts are reported in parts per million relative to an internal standard of residual chloroform (δ = 7.26

ppm for ^{1}H NMR and 77.16 ppm for ^{13}C NMR). For the ^{1}H spectra, data are reported as follows: chemical shift, multiplicity (s = singlet, d = doublet, t = triplet, q = quartet, m = multiplet, and bs = broad singlet), coupling constant in Hz, and integration. Structural assignments were made with additional information from gCOSY, gHSQC, and gHMBC experiments. IR spectra were recorded with a PerkinElmer FT-IR spectrophotometer and are reported in reciprocal centimeters (cm^{-1}). High-resolution mass spectra (HRMS-ESI) were obtained on LCT Waters equipment.

Synthesis of 4 and 9. Compound **4** was prepared starting from 2-bromobenzaldehyde according to the reported procedures.[28] Compound **9** was synthesized according to the published procedure.[30]

Synthesis of Hemicryptophane 10. In a 300 mL mixture of dichloromethane/methanol (1/1), Tris-benzaldehyde phosphine **4** (200 mg, 0.58 mmol) and CTV-NH_2 **9** (300 mg, 0.58 mmol) were combined and stirred at room temperature (20−25 °C) overnight. The reaction mixture was then cooled to 0 °C, and sodium borohydride ($NaBH_4$, 300 mg, 12 equiv) was added gradually with stirring. After a minimum of 4 h, a 10% sodium hydroxide (NaOH) solution (150 mL) was introduced, and stirring was continued overnight. The resulting organic layer was subjected to washing with a 10% NaOH solution (3 × 50 mL), followed by drying over magnesium sulfate. Subsequently, the organic solvent was removed by evaporation. Purification of the crude product was accomplished through silica gel column chromatography using a dichloromethane/methanol (97/3) eluent system, yielding hemicryptophane **10** (170 mg, 35% yield, amorphous solid). ^{1}H NMR (400 MHz, $CDCl_3$, 298 K) δ 7.67−7.63 (m, 3H), 7.33−7.28 (m, 3H), 7.06−6.97 (m, 6H), 6.80 (s, 3H), 6.55−6.51 (m, 3H), 4.74 (d, J = 13.8 Hz, 3H), 4.23 (s, 6H), 3.67 (s, 9H), 3.53 (d, J = 13.8 Hz, 3H), 3.50−3.30 (br, 6H), 2.53 (s, 6H); ^{13}C{^{1}H} NMR (101 MHz, $CDCl_3$, 298 K) δ 149.3, 146.7 (d), 144.8, 144.3 (d), 133.2 (s), 132.2 (2C), 128.9, 127.5 (d), 127.0, 118.4 (br), 113.4, 64.5 (d), 56.2, 50.4 (d), 46.6, 36.2; ^{31}P{^{1}H} NMR (162 MHz, $CDCl_3$, 298 K) δ −40.15; HRMS(ESI-TOF) m/z: $[M + H]^+$ calcd for $C_{51}H_{55}N_3O_6P$ 836.3823 found 836.3820. For COSY, HSQC, and HMBC, see the SI.

Chiral HPLC analysis for (±)-**10**: On a Chiralpak IG column (250 × 4.6 mm), with 1 mL·min^{-1} as flow rate, heptane/EtOH/CH_2Cl_2 (30/30/40) as the mobile phase, UV detection at 254 nm, Rt(*M*-**10**) = 5.6 min, Rt(*P*-**10**) = 8.1 min, k(*M*-**10**) = 0.91, k(*P*-**10**) = 1.76, α = 1.94, and Rs = 4.6.

Resolution of hemicryptophane (±)-**10**: (±)-**10** (67 mg) was dissolved in 5 mL of CH_2Cl_2. On a Chiralpak IG column (250 × 10 mm), with 5 mL.min−1 as flow rate, hexane/EtOH/CH_2Cl_2 (30/30/40) as the mobile phase, UV detection at 254 nm, 50 injections of 100 μL were stacked every 11.8 min. Both enantiomers were collected, and the solvent was then evaporated. The first eluted enantiomer ((+), *M*-**10**, 17 mg) was obtained with 99.5% ee and the second ((−), *P*-**10**, 18 mg) with 98% ee. Ees of the collected fractions were determined on an analytical column.

$$[\alpha]_{589}^{25} = +99(CH_2Cl_2,\ c = 0.19)$$

$$[\alpha]_{589}^{25} = -99(CH_2Cl_2,\ c = 0.19)$$

Synthesis of Hemicryptophane 10@AuCl. A solution of racemic hemicryptophane **10** (45 mg, 0,045 mmol) in 10 mL of dichloromethane at room temperature received a gradual dropwise addition of (Me_2S)AuCl (0.045 mmol, 1 equiv) dissolved in 5 mL of dichloromethane over a period of 30 min. Following an additional 30 min of stirring, the resulting gray solution was filtered through a Celite pad and subsequently evaporated. This process afforded the gold(I) complex hemicryptophane **10**@AuCl in quantitative yield (57 mg, amorphous solid). ^{1}H NMR (400 MHz, $CDCl_3$, 298 K) δ: 7.78 (dd, J = 7.8, 5.6 Hz, 3H), 7.53 (dddd, J = 7.6, 1.4 Hz, 3H), 7.16 (dddd, J = 7.5, 1.5 Hz, 3H), 7.00 (s, 3H), 6.77 (s, 3H), 6.46 (ddd, J = 12.5, 7.8, 1.3 Hz, 3H), 4.66 (d, J = 13.5 Hz, 3H), 4.56 (dd, J = 12.7, 2.3 Hz, 3H), 4.31 (dt, J = 11.0, 7.6 Hz, 3H), 3.82 (ddd, J = 11.5, 8.3, 4.1 Hz, 3H), 3.74 (s, 9H), 3.51 (d, J = 13.6 Hz, 3H), 3.32 (d, J = 12.7 Hz, 3H), 2.82 (dt, J = 10.8, 7.7 Hz, 3H), 2.61 (ddd, J = 11.4, 7.9, 4.0 Hz, 3H). ^{13}C{^{1}H} NMR (101 MHz, $CDCl_3$, 298 K) δ: 150.7, 146.8, 144.3 (d, J = 12.2 Hz), 135.1, 133.2 (d, J = 7.2 Hz), 132.5, 132.5 (d, J = 8.8 Hz), 132.2 (d, J = 2.2 Hz), 128.3 (d, J = 9.4 Hz), 126.2 (d, J = 60.4 Hz), 122.6, 113.7, 74.1, 56.5, 51.6 (d, J = 12.9 Hz), 47.3, 36.3. ^{31}P{^{1}H} NMR (162 MHz, $CDCl_3$, 298 K) δ 1.80. HRMS(ESI-TOF) m/z: $[M + H]^+$ calcd for $C_{51}H_{55}AuClN_3O_6P$ 1068.3177 found 1068.3180. For DEPT135, COSY, NOESY, HSQC, and HMBC, see the SI.

The enantiopure (+)-*P*-**10**@AuCl complex was prepared from the optically resolved (+)-*P*-**10** phosphine following the same procedure as described above.

$$[\alpha]_{589}^{25} = -38(CH_2Cl_2,\ c = 0.34)$$

■ ASSOCIATED CONTENT

Data Availability Statement

The data underlying this study are available in the published article and its Supporting Information.

Supporting Information

The Supporting Information is available free of charge at https://pubs.acs.org/doi/10.1021/acs.joc.3c02984.

^{1}H, ^{13}C{1H}, and ^{31}P NMR spectra and mass spectra of compounds **1**−**10**; HPLC analysis; details on the ECD spectra, crystallographic data (PDF)

Accession Codes

CCDC 2321231 and 2321232 contain the supplementary crystallographic data for this paper. These data can be obtained free of charge via www.ccdc.cam.ac.uk/data_request/cif, or by emailing data_request@ccdc.cam.ac.uk, or by contacting The Cambridge Crystallographic Data Centre, 12 Union Road, Cambridge CB2 1EZ, UK; fax: + 44 1223 336033.

■ ACKNOWLEDGMENTS

The authors thank Michel Giorgi for X-ray structure determination, Marion Jean, Muriel Albalat, and Dr. Nicolas Vanthuyne for the HPLC separation and the ECD mesasurements. This research was supported by the French National Research Agency: ANR Colab, grant number: ANR-19-CE07-0024.

■ REFERENCES

(1) (a) Zhang, D.; Ronson, T. K.; Zou, Y.-Q.; Nitschke, J. R. Metal-organic cages for molecular separations. *Nat. Rev. Chem.* **2021**, *5*, 168−182. (b) Pullen, S.; Tessarolo, J.; Clever, G. H. Increasing structural and functional complexity in self-assembled coordination cages. *Chem. Sci.* **2021**, *12*, 7269−7293. (c) Hardie, M. J. Self-assembled cages and capsules using cyclotriveratrylene-type scaffolds. *Chem. Lett.* **2016**, *45*, 1336−1346. (d) Brotin, T.; Dutasta, J.-P. Cryptophanes and Their Complexes-Present and Future. *Chem. Rev.* **2009**, *109*, 88−130. (e) Xie, H.; Finnegan, T. J.; Gunawardana, V. W. L.; Pavlović, R. Z.; Moore, C. E.; Badjić, J. D. A Hexapodal Capsule for the Recognition of Anions. *J. Am. Chem. Soc.* **2021**, *143*, 3874−3880. (f) Hermann, K.; Ruan, Y.; Hardin, A. M.; Hadad, C. M.; Badjic, J. D. Gated molecular baskets. *Chem. Soc. Rev.* **2015**, *44*, 500−514. (g) Mastalerz, M. Porous Shape-Persistent Organic Cage Compounds of Different Size, Geometry, and Function. *Acc. Chem. Res.* **2018**, *51*, 2411−2422.

(2) (a) Yoshizawa, M.; Klosterman, J. K.; Fujita, M. Functional Molecular Flasks: New Properties and Reactions within Discrete, Self-Assembled Hosts. *Angew. Chem., Int. Ed.* **2009**, *48*, 3418−3438. (b) Zarra, S.; Wood, D. M.; Roberts, D. A.; Nitschke, J. R. Molecular containers in complex chemical systems. *Chem. Soc. Rev.* **2015**, *44*, 419−432. (c) Brown, C. J.; Toste, F. D.; Bergman, R. G.; Raymond, K. N. Supramolecular Catalysis in Metal−Ligand Cluster Hosts. *Chem. Rev.* **2015**, *115*, 3012−3035. (d) Morimoto, M.; Bierschenk, S. M.; Xia, K. T.; Bergman, R. G.; Raymond, K. N.; Dean Toste, F. Advances in supramolecular host-mediated reactivity. *Nat. Catal.* **2020**, *3*, 969−984. (e) Zhang, Q.; Tiefenbacher, K. Terpene cyclization catalysed inside a self-assembled cavity. *Nat. Chem.* **2015**, *7*, 197−202. (f) Leenders, S. H. A. M.; Gramage-Doria, R.; de Bruin, B.; Reek, J. N. H. Transition metal catalysis in confined spaces. *Chem. Soc. Rev.* **2015**, *44*, 433−448. (g) Gaeta, C.; La Manna, P.; De Rosa, M.; Soriente, A.; Talotta, C.; Neri, P. Supramolecular Catalysis with Self-Assembled Capsules and Cages: What Happens in Confined Spaces. *ChemCatChem.* **2021**, *13*, 1638−1658. (h) Roland, S.; Meijide Suarez, J.; Sollogoub, M. Confinement of Metal−N-Heterocyclic Carbene Complexes to Control Reactivity in Catalytic Reactions. *Chem.—Eur. J.* **2018**, *24*, 12464−12473. (i) Olivo, G.; Capocasa, G.; Del Giudice, D.; Lanzalunga, O.; Di Stefano, S. New horizons for catalysis disclosed by supramolecular chemistry. *Chem. Soc. Rev.* **2021**, *50*, 7681−7724. (j) Bete, S. C.; Otte, M. Heteroleptic Ligation by an endo-Functionalized Cage. *Angew. Chem., Int. Ed.* **2021**, *60*, 18582−18586. (k) Otte, M.; Lutz, M.; Klein Gebbink, R. J. M. Selective Synthesis of Hetero-Sequenced Aza-Cyclophanes. *Eur. J. Org. Chem.* **2017**, *2017*, 1657−1661.

(3) Tominaga, M.; Suzuki, K.; Murase, T.; Fujita, M. 24-Fold Endohedral Functionalization of a Self-Assembled M12L24 Coordination Nanoball. *J. Am. Chem. Soc.* **2005**, *127*, 11950−11951.

(4) Murase, T.; Sato, S.; Fujita, M. Nanometer-Sized Shell Molecules That Confine Endohedral Polymerizing Units. *Angew. Chem., Int. Ed.* **2007**, *46*, 1083−1085.

(5) Pluth, M. D.; Bergman, R. G.; Raymond, K. N. Acid catalysis in basic solution: a supramolecular host promotes orthoformate hydrolysis. *Science* **2007**, *316*, 85−88.

(6) Bender, T. A.; Bergman, R. G.; Raymond, K. N.; Toste, F. D. A Supramolecular Strategy for Selective Catalytic Hydrogenation Independent of Remote Chain Length. *J. Am. Chem. Soc.* **2019**, *141*, 11806−11810.

(7) Shi, Q.; Masseroni, D.; Rebek, J. Macrocyclization of Folded Diamines in Cavitands. *J. Am. Chem. Soc.* **2016**, *138*, 10846−10848.

(8) Sun, Q.; Escobar, L.; de Jong, J.; Ballester, P. Self-assembly of a water-soluble endohedrally functionalized coordination cage including polar guests. *Chem. Sci.* **2021**, *12*, 13469−13476.

(9) Wang, Q.-Q.; Gonell, S.; Leenders, S. H. A. M.; Dürr, M.; Ivanović-Burmazović, I.; Reek, J. N. H. Self-assembled nanospheres with multiple endohedral binding sites pre-organize catalysts and substrates for highly efficient reactions. *Nat. Chem.* **2016**, *8*, 225−230.

(10) Yan, X.; Wei, P.; Liu, Y.; Wang, M.; Chen, C.; Zhao, J.; Li, G.; Saha, M. L.; Zhou, Z.; An, Z.; Li, X.; Stang, P. J. Endo- and Exo-Functionalized Tetraphenylethylene M12L24 Nanospheres: Fluorescence Emission inside a Confined Space. *J. Am. Chem. Soc.* **2019**, *141*, 9673−9679.

(11) Henkelis, J. J.; Carruthers, C. J.; Chambers, S. E.; Clowes, R.; Cooper, A. I.; Fisher, J.; Hardie, M. J. Metallo-Cryptophanes Decorated with Bis-N-Heterocyclic Carbene Ligands: Self-Assembly and Guest Uptake into a Nonporous Crystalline Lattice. *J. Am. Chem. Soc.* **2014**, *136*, 14393−14396.

(12) Meng, W.; Breiner, B.; Rissanen, K.; Thoburn, J. D.; Clegg, J. K.; Nitschke, J. R. A self-assembled M8L6 cubic cage that selectively encapsulates large aromatic guests. *Angew. Chem., Int. Ed.* **2011**, *50*, 3479−3483.

(13) Cameron, B. R.; Loeb, S. J.; Yap, G. P. A. Calixarene Metalloreceptors. Synthesis and Molecular Recognition Properties of Upper-Rim Functionalized Calix[4]arenes Containing an Organopalladium Binding Site. *Inorg. Chem.* **1997**, *36*, 5498−5504.

(14) Kaya, Z.; Bentouhami, E.; Pelzer, K.; Armspach, D. Cavity-shaped ligands for asymmetric metal catalysis. *Coord. Chem. Rev.* **2021**, *445*, No. 214066.

(15) Perraud, O.; Sorokin, A. B.; Dutasta, J.-P.; Martinez, A. Oxidation of cycloalkanes by H_2O_2 using a copper−hemicryptophane complex as a catalyst. *Chem. Commun.* **2013**, *49*, 1288−1290.

(16) Martinez, A.; Dutasta, J.-P. Hemicryptophane−oxidovanadium-(V) complexes: Lead of a new class of efficient supramolecular catalysts. *J. Catal.* **2009**, *267*, 188−192.

(17) Ikbal, S. A.; Colomban, C.; Zhang, D.; Delecluse, M.; Brotin, T.; Dufaud, V.; Dutasta, J.-P.; Sorokin, A. B.; Martinez, A. Bioinspired Oxidation of Methane in the Confined Spaces of Molecular Cages. *Inorg. Chem.* **2019**, *58*, 7220−7228.

(18) Qiu, G.; Nava, P.; Martinez, A.; Colomban, C. A tris-(benzyltriazolemethyl)amine-based cage as a CuAAC ligand tolerant to exogeneous bulky nucleophiles. *Chem. Commun.* **2021**, *57*, 2281−2284.

(19) Matt, D.; Harrowfield, J. Phosphines and other P(III)-derivatives with Cavity-shaped Subunits: Valuable Ligands for Supramolecular Metal Catalysis, Metal Confinement and Subtle Steric Control. *ChemCat Chem.* **2021**, *13*, 153−168.

(20) Izzet, G.; Zeng, X.; Over, D.; Douziech, B.; Zeitouny, J.; Giorgi, M.; Jabin, I.; Le Mest, Y.; Reinaud, O. First Insights into the Electronic Properties of a Cu(II) Center Embedded in the PN_3 Cap of a Calix[6]arene-Based Ligand. *Inorg. Chem.* **2009**, *48*, 4317−4330.

(21) Raytchev, P. D.; Perraud, O.; Aronica, C.; Martinez, A.; Dutasta, J.-P. A New Class of C_3-Symmetrical Hemicryptophane Hosts: Triamide- and Tren-hemicryptophanes. *J. Org. Chem.* **2010**, *75*, 2099−2102.

(22) Zhang, D.; Cochrane, J. R.; Di pietro, S.; Guy, L.; Gornitzka, H.; Dutasta, J.-P.; Martinez, A. Breathing" Motion of a Modulable Molecular Cavity. *Chem.—Eur. J.* **2017**, *23*, 6495−6498.

(23) Qiu, G.; Colomban, C.; Vanthuyne, N.; Giorgi, M.; Martinez, A. Chirality transfer in a cage controls the clockwise/anticlockwise propeller arrangement of the tris(2-pyridylmethyl)amine ligand. *Chem. Commun.* **2019**, *55*, 14158−14161.

(24) Perraud, O.; Robert, V.; Martinez, A.; Dutasta, J.-P. A Designed Cavity for Zwitterionic Species: Selective Recognition of Taurine in Aqueous Media. *Chem.—Eur. J.* **2011**, *17*, 13405−13408.

(25) Chatelet, B.; Gornitzka, H.; Dufaud, V.; Jeanneau, E.; Dutasta, J.-P.; Martinez, A. Superbases in Confined Space: Control of the Basicity and Reactivity of the Proton Transfer. *J. Am. Chem. Soc.* **2013**, *135*, 18659−18664.

(26) Chatelet, B.; Dufaud, V.; Dutasta, J.-P.; Martinez, A. Catalytic Activity of an Encaged Verkade's Superbase in a Base-Catalyzed Diels–Alder Reaction. *J. Org. Chem.* **2014**, *79*, 8684–8688.
(27) Whitnall, M. R.; Hii, K. K.; Thornton-Pett, M.; Kee, T. P. Conformational diastereoisomerism in tris-(2-alkylimino) triphenylphosphines. *J. Organomet. Chem.* **1997**, *529*, 35–50.
(28) Chatelet, B.; Payet, E.; Perraud, O.; Dimitrov-Raytchev, P.; Chapellet, L.-C.; Dufaud, V.; Martinez, A.; Dutasta, J.-P. Shorter and Modular Synthesis of Hemicryptophane-tren Derivatives. *Org. Lett.* **2011**, *13*, 3706–3709.
(29) Long, A.; Perraud, O.; Albalat, M.; Robert, V.; Dutasta, J.-P.; Martinez, A. Helical Chirality Induces a Substrate-Selectivity Switch in Carbohydrates Recognitions. *J. Org. Chem.* **2018**, *83*, 6301–6306.
(30) Long, A.; Jean, M.; Albalat, M.; Vanthuyne, N.; Giorgi, M.; Górecki, M.; Dutasta, J.-P.; Martinez, A. Synthesis, resolution, and chiroptical properties of hemicryptophane cage controlling the chirality of propeller arrangement of a C_3 triamide unit. *Chirality* **2019**, *31*, 910–916.
(31) (a) Schmitt, A.; Perraud, O.; Payet, E.; Chatelet, B.; Bousquet, B.; Valls, M.; Padula, D.; Di Bari, L.; Dutasta, J.-P.; Martinez, A. Improved hemicryptophane hosts for the stereoselective recognition of glucopyranosides. *Org. Biomol. Chem.* **2014**, *12*, 4211–4217. (b) Perraud, O.; Dimitrov-Raytchev, P.; Martinez, A.; Dutasta, J.-P. Chirality, Resolution and absolute configuration assignment of a chiral hemicryptophane molecular cage. *Chirality* **2010**, *22*, 885–888. (c) Cochrane, J. R.; Schmitt, A.; Wille, U.; Hutton, C. A. Synthesis of cyclic peptide hemicryptophanes: enantioselective recognition of a chiral zwitterionic guest. *Chem. Commun.* **2013**, *49*, 8504–8506. (d) Canceill, J.; Collet, A.; Gabard, J.; Gottarelli, G.; Spada, G. P. Exciton approach to the optical activity of C_3-cyclotriveratrylene derivative. *J. Am. Chem. Soc.* **1985**, *107*, 1299–1308. (e) Canceill, J.; Collet, A.; Gottarelli, G.; Palmieri, P. Synthesis and exciton optical activity of D_3-cryptophanes. *J. Am. Chem. Soc.* **1987**, *109*, 6454–6464.
(32) (a) Escayola, S.; Bahri-Laleh, N.; Poater, A. %VBur index and steric maps: from predictive catalysis to machine learning Muratov. *Chem. Soc. Rev.* **2024**, *53*, 853–882. (b) K; Gagosz, F. Confinement-Induced Selectivities in Gold(I) Catalysis—The Benefit of Using Bulky Tri-(ortho-biaryl)phosphine Ligands. *Angew. Chem.* **2022**, *61*, No. e202203452.